



1 Imprint of eutrophication on methane-cycling microbes in freshwater sediment
2
3 Alice Bosco-Santos^{1*}, Eulalie Rose Beyala Bekono¹, Santona Khatun¹, Marie-Ève
4 Monchamp², Joana Séneca^{3,4}, Petra Pjevac^{3,4}, Jasmine S. Berg¹
5 ¹Institute of Earth Surface Dynamics (IDYST), University of Lausanne, Lausanne, Switzerland
6 ²Biology Department, McGill University, Montreal, Canada
7 ³Division of Microbial Ecology, Centre for Microbiology and Environmental Systems Science,
8 University of Vienna, Vienna, Austria
9 ⁴Joint Microbiome Facility of the Medical University of Vienna and the University of Vienna,
10 Vienna, Austria
11 [*\(alice.boscasantos@unil.ch\)](mailto:alice.boscasantos@unil.ch)

12
13
14
15
16
17
18
19
20
21
22
23
24
25
26
27
28
29
30
31
32
33



34 **Abstract.** Eutrophication can alter methane (CH₄) cycling in lakes, yet its long-term effect on
35 sediment microbial communities remains unclear. To elucidate these effects, we analyzed a
36 400-year-old sediment record from the historically eutrophied Lake Joux, Switzerland,
37 combining porewater and solid-phase geochemistry with 16S rRNA gene amplicon analyses.
38 Lithological and chemical stratification defined three intervals (deep eutrophic, middle
39 carbonate, upper eutrophic) that were correlated with changes in organic matter sources.
40 Methanogens were clearly depth-partitioned: methylotrophic Methanomassiliicoccales
41 dominated deep eutrophic sediments, whereas hydrogenotrophic Methanomicrobiales and
42 Methanobacteriales increased upward in shallower, more recent sediments with fresher organic
43 matter. Paired isotopic data support this substrate-driven shift in CH₄ production. Although O₂
44 was not detected below ~0.4 cm, sequences of aerobic gammaproteobacterial methanotrophs
45 (*Crenothrix* and *Methylobacter*) were abundant in surface sediments down to ~20 cm sediment
46 depth, correlating with NO₃⁻ and PO₄³⁻ concentrations. The absence of anaerobic
47 methanotrophs and C-isotopic evidence for ongoing methane oxidation suggest that these O₂-
48 requiring, methane monooxygenase-utilizing Methylococcales constitute the dominant CH₄
49 sink in these surface sediments. These findings reveal that eutrophication can cause a
50 stratification of methane-cycling microbial communities, highlighting the role of sedimentary
51 legacies in regulating benthic CH₄ emissions from freshwater ecosystems.

52
53
54
55
56
57
58
59
60
61
62
63
64



65 1. Introduction

66 Freshwater ecosystems are significant sources of the greenhouse gas methane (CH_4),
 67 with natural lakes estimated to contribute more than 70% to freshwater CH_4 emissions (Sanches
 68 et al., 2019). Despite their substantial contribution to atmospheric CH_4 , the mechanisms
 69 regulating CH_4 emissions from lakes at regional and global scales remain poorly understood
 70 (Bastviken et al., 2011; Sanches et al., 2019). In freshwater sediments, CH_4 is abundantly
 71 produced via anaerobic methanogenesis by archaea (Bastviken et al., 2004; Bastviken et al.,
 72 2011; Conrad, 2020; Dean et al., 2018; Saunio et al., 2020; Tranvik et al., 2009). Methanogens
 73 can respire different substrates produced during organic matter remineralization and are
 74 classified according to three known pathways for CH_4 production: hydrogenotrophic (carbon
 75 dioxide reduction using hydrogen), acetoclastic (splitting acetate), and methylotrophic (using
 76 methylated compounds like methanol) (Garcia et al., 2000). Environmental factors such as
 77 substrate concentration, temperature, salinity, and pH influence the predominance of these
 78 pathways, with methylotrophic methanogenesis, for instance, being favored at higher salinity
 79 and acidity (Bueno De Mesquita et al., 2023; Yvon-Durocher et al., 2014).

80 Much of the CH_4 produced in lake sediments is oxidized through both aerobic and
 81 anaerobic microbial processes before it can reach the atmosphere (Bastviken et al., 2004;
 82 Bastviken et al., 2008; Martinez-Cruz et al., 2017; Martinez-Cruz et al., 2018; Oswald et al.,
 83 2016). Aerobic oxidation, predominantly performed by methane-oxidizing bacteria (MOB)
 84 from the Gammaproteobacteria and Alphaproteobacteria classes, occurs at the sediment-water
 85 interface and in the water column (Hanson and Hanson, 1996; Knief, 2015). MOB rely on the
 86 O_2 -dependent methane monooxygenase enzymes to oxidize up to 90% of sediment-derived
 87 CH_4 , thus helping to mitigate greenhouse gas emissions from freshwater ecosystems (Bastviken
 88 et al., 2004; Bastviken et al., 2008). Anaerobic oxidation of methane (AOM) is performed by
 89 methanotrophic archaea (ANMEs), often in partnership with bacteria that use electron
 90 acceptors other than oxygen (Knittel and Boetius, 2009; Milucka et al., 2012; Wegener et al.,
 91 2015). In marine environments where sulfate concentrations are high, sulfate-AOM is the
 92 dominant process (Jørgensen et al., 2001; Wegener and Boetius, 2009). In contrast, the electron
 93 acceptors sulfate, nitrate/nitrite, humic substances, and diverse metal oxides contribute in
 94 various degrees to AOM in freshwater sediments (Chen et al., 2023; Deutzmann and Schink,
 95 2011; Martinez-Cruz et al., 2018; Zhao et al., 2024).

96 Recently, it has been proposed that eutrophication induced by anthropogenic nutrient
 97 inputs (e.g., nitrates and phosphates) into lake ecosystems influences methanogen and
 98 methanotroph community structure by altering organic matter quality and quantity (Beaulieu



99 et al., 2019; Yang et al., 2021; Yang et al., 2019; Yang et al., 2020; Zhu et al., 2022). The influx
 100 of organic carbon from phytoplankton blooms enhances organic matter mineralization in lake
 101 bottom waters and sediments, depleting electron acceptors such as oxygen (O_2), nitrate (NO_3^-
 102), sulfate (SO_4^{2-}), and metal oxides (Fe(III), Mn(IV)). The decomposition of phytoplankton
 103 biomass also releases significant amounts of methyl-sulfur compounds, favoring
 104 methylophilic CH_4 production (Penger et al., 2012; Tebbe et al., 2023; Tsola et al., 2021; Yan
 105 et al., 2017; Zhou et al., 2022). Anaerobic conditions, combined with increased organic matter
 106 availability, are expected to boost methanogenesis, resulting in elevated CH_4 release following
 107 eutrophication (Fiskal et al., 2019; Sanches et al., 2019; Zhou et al., 2022).

108 Conversely, nutrient addition can stimulate microbial CH_4 oxidation (Yang et al., 2019).
 109 Some aerobic MOB can oxidize CH_4 while respiring NO_3^- (denitrification), and a growing body
 110 of evidence supports the widespread occurrence and activity of these bacteria in O_2 -limited
 111 environments (Almog et al., 2024; Kits et al., 2015; Reis et al., 2024; Schorn et al., 2024).
 112 Importantly, MOB exhibit niche partitioning along O_2 - CH_4 and nutrients gradients with
 113 Gammaproteobacteria, Alphaproteobacteria, and nitrite-dependent taxa that produce O_2
 114 intracellularly, such as *Candidatus Methylophilus*, occupying distinct layers (Mayr et al.,
 115 2020; Reis et al., 2020). Gammaproteobacterial MOB are generally associated with fast-
 116 growing life strategies in resource-rich conditions, whereas alphaproteobacterial MOB are
 117 adapted to resource-limited or stable environments (Ho et al., 2013). Indeed, P and N
 118 enrichment, for instance, can increase CH_4 oxidation rates and favor Gammaproteobacteria
 119 over Alphaproteobacteria MOB (Nijman et al., 2022; Veraart et al., 2015). Together, these
 120 findings highlight that nutrients modulate both CH_4 production and consumption, adding
 121 complexity to how eutrophication shapes lacustrine CH_4 dynamics (Nijman et al., 2022; Reis
 122 et al., 2020; Veraart et al., 2015; Wei et al., 2022).

123 Eutrophication of lakes in Switzerland reached critical levels during the mid-20th
 124 century, particularly in the 1970s, due to rapid industrialization, urbanization, and agricultural
 125 intensification. Public outcry and scientific research prompted the introduction of wastewater
 126 treatment plants and stricter regulations on phosphate detergents, leading to significant
 127 improvements in water quality by the late 20th century. Nevertheless, sediments retain a legacy
 128 of this eutrophication in the form of increased organic matter content (Fiskal et al., 2019),
 129 which continues to shape microbial community structure (Han, 2020) long after lake waters
 130 recovered. Some studies have reported clear vertical zonation of methanogenic and
 131 methanophilic communities in relation to trophic history and electron acceptor distributions
 132 (Rissanen et al., 2023; Van Grinsven et al., 2022), while others found little to no stratification



133 (Meier et al., 2024). Consequently, the cascading impacts of anthropogenic nutrient inputs on
 134 the balance of CH₄ production and oxidation in lake sediments remain poorly constrained.

135 To address this knowledge gap, we focused on the sedimentary record of Lake Joux
 136 (Vaud, Switzerland), a site with a well-documented history of trophic regime shifts and
 137 phytoplankton bloom deposits (Lavrieux et al., 2017; Monchamp et al., 2021). We combined
 138 microbial community sequencing with isotopic analyses of different carbon pools in lake
 139 sediments dating back to the 16th century. The isotopic behavior of the two stable carbon
 140 isotopes, ¹²C and ¹³C, plays a critical role in understanding microbial CH₄ production and
 141 consumption, as ¹²C is preferentially used over ¹³C due to its lighter mass and greater reactivity.
 142 During methanogenesis, CH₄ produced is typically depleted in ¹³C relative to precursor
 143 substrates such as organic matter or CO₂, resulting in isotopically lighter CH₄ (Conrad, 2005).
 144 Conversely, methanotrophs preferentially oxidize ¹²CH₄, enriching the residual CH₄ pool in ¹³C
 145 and simultaneously generating isotopically lighter dissolved inorganic carbon (δ¹³C_{DIC})
 146 (Barker and Fritz, 1981; Jahnke et al., 1999; Templeton et al., 2006; Whiticar, 1999). Thus,
 147 this carbon isotope fractionation provides key insights into the microbial processes driving CH₄
 148 cycling, enabling inference of microbial activity even without direct rate measurements (Blaser
 149 and Conrad, 2016; Conrad, 2005, 2007; Valentine et al., 2004).

150 **2. Materials and methods**

151 **2.1 Study Area**

152 Lake Joux is a perialpine lake in the Joux Valley in the Swiss Jura Mountains (Fig. 1).
 153 The valley developed in a Jura syncline, marked by glacial erosion and Quaternary deposits,
 154 and it lies mainly on Upper Jurassic and Tertiary limestones. The lake has an average depth of
 155 32 m, a surface area of approximately 9 km² (maximum 9 km in length and 1 km in width), and
 156 a watershed covering around 211 km². Situated at an altitude of 1,183 meters, the lake is subject
 157 to intense seasonal variations and meteorological events, which drive the runoff of both natural
 158 and anthropogenic materials.

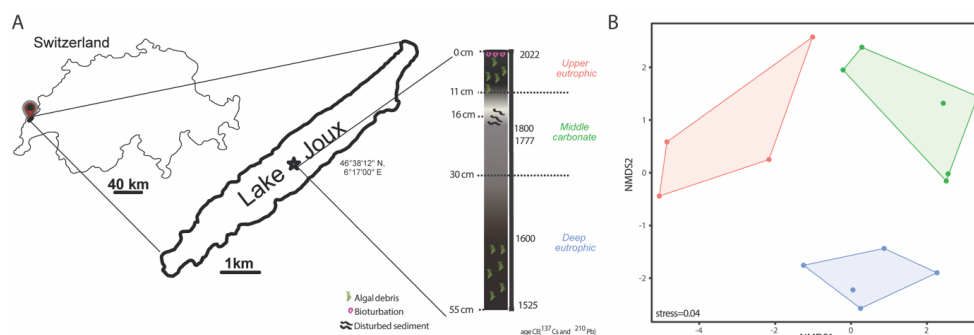
159 Human activity in the watershed dates back over 6,850 years (Lavrieux et al., 2017;
 160 Mitchell et al., 2001; Monchamp et al., 2021). By the 16th century, the area around Lake Joux
 161 became more densely populated, leading to land drainage and deforestation for livestock
 162 farming (Piguet, 1946). Frequent crop failures and food shortages during the late 17th century
 163 spurred the growth of glassmaking and lapidary industries. Horology, introduced in the 18th
 164 century, became the region's dominant economic activity by the 19th century. This period of



165 industrialization resulted in a transition from cultivated farmland to pastures and fallow fields
 166 (Lavrieux et al., 2017).

167 Agricultural intensification and urban expansion during the 20th century significantly
 168 increased nutrient inputs to Lake Joux, resulting in pronounced eutrophication. Phosphorus
 169 levels peaked at 35 µg/L in 1979 (Lods-Crozet et al., 2006), triggering major ecological
 170 changes, including rapid shifts in phytoplankton communities as eutrophication-adapted taxa
 171 outcompeted the lake's original species (Monchamp et al., 2021). A re-oligotrophication phase
 172 began in 1988–1989 following improved nutrient management and mitigation efforts.
 173 However, despite these reductions in external nutrient loading, the lake has not returned to its
 174 pre-eutrophication conditions. More than 70 years after the documented episode of
 175 eutrophication, the water column remains altered, suggesting that the system has shifted to an
 176 alternative stable state with a biological configuration resistant to reversal (Lods-Crozet et al.,
 177 2006; Monchamp et al., 2021).

178



179

180 **Figure 1** - Schematic representation and geographic coordinates of where the sediment cores
 181 from Lake Joux, Switzerland, were sampled in 2023. The 55 cm sedimentary profile has three
 182 distinct stratigraphic layers: deeper eutrophic, middle carbonate, and upper eutrophic.

183

184 2.2 Sampling

185 In 2023, three gravity cores (45-55 cm long) were recovered from Lake Joux's lakebed
 186 using a Uwitec gravity corer. The cores were taken from one of the deepest parts of the lake
 187 (46°38'12" N, 6°17'00" E; 28 m depth) and sealed with rubber caps. One core was pre-drilled
 188 and taped at 3 cm intervals to facilitate rapid CH₄ sampling using 3 ml syringes on shore. The
 189 other two cores, one for porewater and the other for sediment chemistry and microbiome
 190 analyses, were processed in the laboratory within 24 h. Porewater was extracted via N₂ flushed
 191 syringes attached to 0.2 µm Rhizons (Rhizosphere), inserted every 3 cm along the core, stored



at 4°C and analyzed within 48 h. The third sediment core was opened with a handheld saw and sectioned every 3 cm. Each sample was split into an acid-cleaned vial and a sterile vial, then frozen at -20°C.

2.3 Porewater chemistry

Samples for dissolved anions (PO_4^{3-} , NO_3^- , SO_4^{2-}) were transferred to plastic vials while flushing with N_2 , capped, and analyzed using an ion chromatograph (DX-ICS-1000, DIONEX) equipped with an AS11-HC column. Dissolved inorganic carbon (DIC) porewater samples were filled into 1.5 ml borosilicate vials and capped without headspace to prevent CO_2 degassing. To measure $\delta^{13}\text{C}_{\text{DIC}}$, samples were transferred to helium-flushed Exetainers containing 200 μL of 85% phosphoric acid, converting all DIC to CO_2 . The CO_2 in the headspace was then analyzed using a GasBench II (ThermoFisher Scientific) coupled with an isotope ratio mass spectrometer (Delta V, ThermoFisher Scientific). Carbon isotopes are reported in the conventional delta notation relative to the Vienna Pee Dee Belemnite (VPDB) standard.

For dissolved sulfide analysis, porewater was fixed with 0.05 M Zn-acetate ($\text{Zn}(\text{CH}_3\text{COO})_2 \cdot 2\text{H}_2\text{O}$) solution at a 1:2 ratio immediately after extraction, and dissolved sulfide was quantified photometrically using the methylene blue method (Cline, 1969).

2.4 Sediment description and chemistry

Sediment from the opened core was visually assessed (using standard charts) for color and granulometry based on observable differences in particle size, texture, and sorting within the sediment layers.

For total phosphorus (P), ~1 g of wet sediment was digested in 9 ml of 4:2 HNO_3 :HCl using an Anton Paar microwave system, filtered (0.45 μm glass fiber), and analyzed by ICP-OES (Agilent 5800). Calibration used a multi-element standard, with certified reference materials yielding 85–102% recovery.

Elemental C, N, H, and S were measured on 1–3 mg of freeze-dried sediment using a UNICUBE (Elementar®) at EPFL's ISIC-MSEAP. TOC and TIC were estimated via loss on ignition (500°C and 1200°C). $\delta^{13}\text{C}_{\text{Org}}$ was determined by EA-Isolink IRMS (Thermo Fisher) after 48 h treatment with 6 N HCl to remove carbonates. Results are reported in delta notation (VPDB), with a reproducibility better than 0.2‰.



224 Acid-volatile sulfur (AVS) and chromium-reducible sulfur (CRS) were extracted from
 225 1–2 g of frozen sediment as per Spangenberg and Bosco-Santos (2024). Sulfide in AVS and
 226 CRS fractions was measured colorimetrically (Cline, 1969) and CRS sulfur isotopic
 227 composition ($\delta^{34}\text{S}_{\text{CRS}}$) by IRMS (Spangenberg and Bosco-Santos, 2024). These measurements
 228 help distinguish easily mobilized sulfide pools (AVS) from more stable sulfur forms (CRS) in
 229 sediments.

230

231 2.5 Dissolved oxygen and methane

232 Oxygen concentrations were measured using a 200 μm -tip glass microsensor
 233 (Unisense) after 2-point calibration in Na-dithionite and air-saturated water. Vertical profiles
 234 were recorded at 250 μm steps with a motorized controller and Field Multimeter (Unisense).

235 For CH_4 analysis, 3 cm^3 of sediment was transferred into 100 ml serum bottles with 5
 236 ml of 10% NaOH, sealed, and homogenized. Dissolved CH_4 was extracted by headspace
 237 displacement and quantified via gas chromatography (Joint Analytical Systems) at Eawag.
 238 $\delta^{13}\text{C}_{\text{CH}_4}$ was measured using GCC-IRMS (Agilent 6890N with Thermo Finnigan IRMS) and
 239 analyzed with IonVantage software (Khatun et al., 2024). Results are reported in delta notation
 240 relative to VPDB with an analytical error $<1.1\%$.

241 Carbon isotopic fractionation factors (α) between C_{org} (substrate) and CH_4 (product)
 242 were as: $\alpha = (\delta^{13}\text{C}_{\text{org}} + 1000)/(\delta^{13}\text{C}_{\text{CH}_4} + 1000)$. The corresponding isotopic fractionation (ϵ , ‰)
 243 was then determined by the relationship $\epsilon = (\alpha - 1) \times 1000$, allowing interpretation of trends in
 244 dominant methanogenic pathways.

245

246 2.6 DNA extraction and 16S rRNA gene amplicon analysis

247 DNA was extracted from Lake Joux sediments using the PowerSoil Pro Kit (Qiagen).
 248 Extraction, sequencing, and raw data processing were conducted at the Joint Microbiome
 249 Facility (Medical University of Vienna and University of Vienna; project ID JMF-2310-14).
 250 The V4 hypervariable region of the 16S rRNA gene was amplified and sequenced to assess the
 251 total microbial diversity in the collected samples. Amplification was performed with linker-
 252 modified 515F and 806R (Apprill et al., 2015; Parada et al., 2016) primers, and amplicons were
 253 barcoded, multiplexed, sequenced on an Illumina MiSeq (v3 chemistry, 2x 300 bp), and
 254 extracted from the raw sequencing data as described in detail in Pjevac et al. (2021). Amplicon
 255 Sequence Variants (ASVs) were inferred using the DADA2 R package v1.42 (Callahan et al.,
 256 2016b), applying the recommended workflow (Callahan et al., 2016a). FASTQ reads 1 and 2



257 were trimmed at 220 nt and 150 nt with allowed expected errors of 2. ASV sequences were
 258 subsequently classified using DADA2 and the SILVA database SSU Ref NR 99 release 138.1
 259 (Quast et al., 2012; McLaren and Callahan, 2021) using a confidence threshold of 0.5. ASVs
 260 without classification or classified as eukaryotes, mitochondria, or chloroplasts, as well as well-
 261 known buffer contaminations, were removed. After filtering, only samples with at least 7000
 262 read pairs were kept for further analyses. The relative abundance of chloroplast sequences was
 263 examined separately to assess phytoplankton debris across the sediment profile.

264 Downstream analyses were performed using R v4.3.2 and Bioconductor v3.16
 265 packages SummarizedExperiment v1.32, SingleCellExperiment v1.24,
 266 TreeSummarizedExperiment v2.8 (Huang et al., 2021), mia v1.8
 267 (<https://github.com/microbiome/mia>), LMDist (Hoops and Knights, 2023), vegan 2.6-8,
 268 phyloseq v1.44 (McMurdie and Holmes, 2013) (Vegan R package; phyloseq R package),
 269 microbiome v1.22 (<http://microbiome.github.io>), microViz v0.10.8 (Barnett et al., 2021), and
 270 corrrplot (Wei, 2024). In order to determine sediment zonation by environmental variables, we
 271 performed non-metric multidimensional scaling (NMDS) on a Euclidean distance matrix of z-
 272 scored environmental data for samples between 0.5 and 43.5 cm sediment depth, using the
 273 function metaMDS() in the R package vegan. The NMDS stress value was 0.04. Microbial
 274 community alpha diversity indices were calculated on rarified 16S rRNA gene amplicon data
 275 using R packages vegan and mia. For community dissimilarity analysis, microbial 16S rRNA
 276 gene amplicon sequence count data was centered log ratio (CLR) transformed, a pairwise
 277 Aitchison distances matrix was computed, and oversaturated distances in the dissimilarity
 278 matrix were corrected and smoothed using LMDist with default settings prior to ordination
 279 using principal coordinates analysis (PCoA). To identify the environmental variables that
 280 significantly contributed to the variation in microbial community structure, correlations
 281 between microbial community composition and environmental variables were assessed using
 282 Mantel tests, based on Euclidean distances calculated from Z-score standardized environmental
 283 variables and LMDist corrected and smoothed Aitchison distances of 16S rRNA gene amplicon
 284 sequencing data. Prior to correlation analysis, five samples from the deep eutrophic layer
 285 without corresponding environmental data were excluded. Mantel tests were performed using
 286 Spearman's rank correlation as implemented in the R package vegan. The resulting p-values
 287 were adjusted for multiple testing using the false discovery rate (FDR) method. Highly
 288 correlated environmental variables (Spearman's $r > 0.8$, Figure S1), as assessed by the function
 289 cor() in the R package corrrplot, were removed before the Mantel tests.

290



291 **3. Results**

292 **3.1 Sediment description**

293 The 55-cm deep sediment record of Lake Joux could be classified into three main
294 intervals based on distinct lithological and chemical features (Fig. 1 and Supplementary Fig.
295 1). The 'deep eutrophic' interval, from 55 cm to 30 cm, comprises black and silty sediments,
296 indicating a period of higher lake productivity and low oxygen conditions. Occasional fine sand
297 and organic fibers are also present. In the 'middle carbonate' interval, from 30 cm to 11 cm, the
298 sediments transition from a murky gray with heterogeneous brownish features, suggesting
299 changes in organic matter quality and oxidation states (Fig. 1) to whitish silty-sandy sediments,
300 with the contribution of shells above 13.5 cm, indicating the dominant deposition of carbonates
301 (Fig. 1). The 'upper eutrophic' interval, from 11 cm to 0 cm, contains intensely black sediment
302 with frequent plant debris, reflecting recent environmental changes.

303 To assign approximate ages to our sedimentary profile, we correlated our lithological
304 intervals to other Lake Joux sedimentary sequences previously published and dated using ^{237}Cs
305 and ^{210}Pb (Lavrieux et al., 2017; Magny et al., 2008) (Fig. 1). This correlation places the base
306 of our core, the deep eutrophic interval, in the late 16th century (middle-upper U3 of Lavrieux
307 et al., 2017). Reported sedimentation rates were 0.04 - 0.11 cm/yr until the end of the middle
308 carbonate interval, when they increased to a short-lived peak of ~ 0.83 cm/yr near the late 18th
309 century, and then declined to an average of 0.18 cm/yr over the past 60 years in the upper
310 eutrophic interval (Lavrieux et al., 2017).

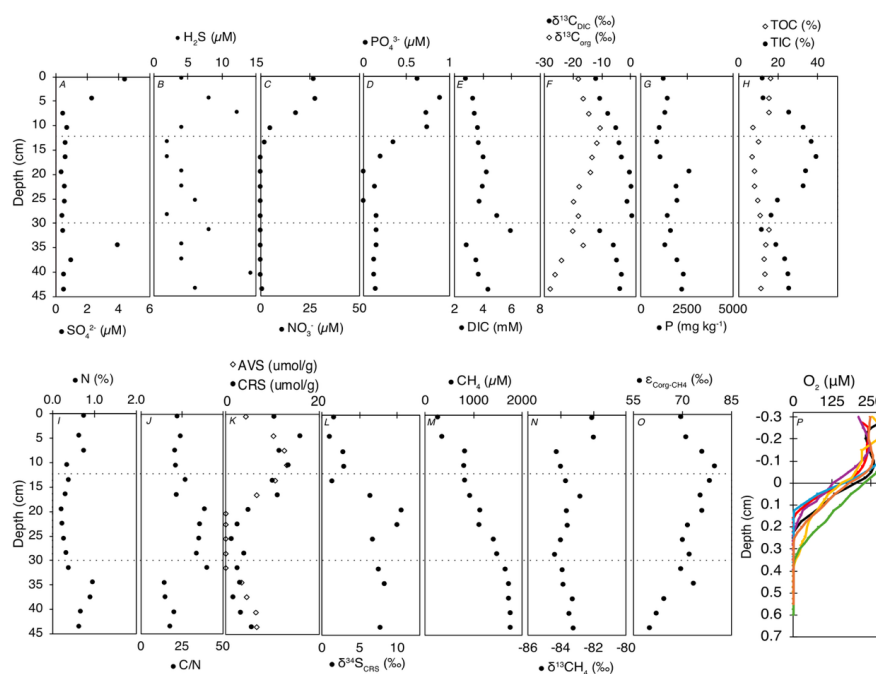


Figure 2 - Geochemical profiles of porewater, solid-phase compounds, and dissolved gases in Lake Joux sediments. Dashed lines represent the interpreted intervals corresponding to 'deep eutrophic' from 55 to 30.5 cm; 'middle carbonate' from 28.5 to 11 cm; and 'upper eutrophic' from 11 to 0 cm. All data are available in Supplementary Material Table 1 (panels A to N) and Table 2 (panel O).

3.2 Porewater chemistry

Sulfate (SO_4^{2-} , between 0.35 μM and 4.5 μM) and dissolved sulfide (H_2S , between 2 μM and 14.3 μM) were measurable throughout the entire sedimentary profile, with peak concentrations in deep eutrophic sediments around 40 cm and again in the upper eutrophic sediments around 7.5 cm depth (Fig. 2A and 2B).

Dissolved nitrate (NO_3^-) and phosphate (PO_4^{3-}) first appeared at 19.5 cm and 16.5 cm, respectively, with concentrations progressively increasing toward the surface, reaching maximum values of 27 μM for NO_3^- and 0.62 μM for PO_4^{3-} (Fig. 2C and 2D).

Dissolved inorganic carbon (DIC) concentrations with isotopically heavier composition ($\delta^{13}\text{C}_{\text{DIC}}$) were highest in the middle carbonate interval between 16.5 cm and 31.5 cm (Fig. 2E). Above 7.5 cm depth, $\delta^{13}\text{C}_{\text{DIC}}$ values progressively became lighter toward the surface, reaching a minimum of -12‰ (Fig. 2F).



330

331 **3.3 Sediment chemistry**

332 **3.3.1 Phosphorous and organic matter characterization**

333 Total phosphorus (P) content, ranging from 860 to 2612 mg kg⁻¹, was generally higher
 334 in the deeper sediments and progressively decreased towards the surface, except for a sharp
 335 peak at 19.5 cm depth (Fig. 2G). Organic carbon (TOC) exhibited higher concentrations in both
 336 the deep eutrophic and upper eutrophic sediments, contrasting with TIC content, which peaked
 337 in the middle carbonate interval (Fig. 2H). The $\delta^{13}\text{C}_{\text{org}}$ was lightest in the deep eutrophic
 338 sediments (-28.22‰ at 43.5 cm) and heaviest in the upper eutrophic sediments (-10.76‰ at
 339 10.5 cm) (Fig. 2F).

340 Nitrogen content followed the same pattern as TOC, with higher N in the deep and
 341 upper eutrophic sediments compared to the middle carbonate region (Fig. 2I). The ratio
 342 between C and N, a qualitative parameter of organic matter source (Meyers, 1994), exhibited
 343 relatively lower values in the deep eutrophic sediments, increasing in the middle carbonate
 344 sediments and decreasing again in the upper eutrophic sediments (Fig. 2J).

345

346 **3.3.2 Solid-phase sulfides**

347 Acid volatile sulfides (AVS) were measurable in the deep eutrophic sediments between
 348 43.5 and 34.5 cm and within the upper eutrophic sediments above 19.5 cm depth. The
 349 maximum concentrations of AVS in the upper eutrophic sediments (around 418 $\mu\text{g kg}^{-1}$ at 10.5
 350 cm) were about twice as high as in deep eutrophic sediments (200 $\mu\text{g kg}^{-1}$ at 40.5 cm) (Fig.
 351 2K). Chromium reducible sulfur (CRS) also exhibited higher concentrations in the shallower
 352 sediments, becoming more prominent from 16.5 cm depth to the surface. CRS concentrations
 353 were more variable than AVS, varying from 23 $\mu\text{g kg}^{-1}$ to 510 $\mu\text{g kg}^{-1}$ (Fig. 2K). The isotopic
 354 composition $\delta^{34}\text{S}$ of CRS was positive throughout the profile, ranging from ~1‰ near the
 355 surface to a maximum of 10.5‰ at 19.5 cm depth. Values remained elevated in the middle
 356 carbonate and deep eutrophic zones (e.g., 8.3‰ at 34.5 cm and 7.7‰ at 43.5 cm), indicating
 357 that the reduced sulfur pool is isotopically enriched in ³⁴S across the sediment column (Fig.
 358 2L).

359

360 **3.3.3 Dissolved oxygen and methane**

361 Methane (CH₄) concentrations were highest in the deep eutrophic sediments, with a
 362 maximum of approximately 1760 μM at 45 cm depth. From 31.5 cm depth, CH₄ exhibited a



363 clear decreasing trend, reaching the lowest concentration (253 μM) at the surface (Fig. 2M).
 364 The most significant drop in CH_4 concentrations occurred between 7.5 and 4.5 cm depth, where
 365 the concentrations decreased by half (Fig. 2M). The $\delta^{13}\text{C}_{\text{CH}_4}$ exhibited minimal variation along
 366 the profile, averaging $-83.0 \pm 0.7\text{‰}$. The most pronounced isotopic shift ($>2.2\text{‰}$) towards
 367 heavier values occurred at the same depth as the sharp decline in CH_4 concentration (Fig. 2N).

368 Fractionation factors (α) between C_{org} and CH_4 ranged from 1.069 to 1.080 across
 369 sediment depths, corresponding to carbon isotope fractionations (ϵ) of 69‰ to 80‰ (Fig. 2O).
 370 These values reflect the measurable discrimination between ^{13}C and ^{12}C during CH_4 production
 371 from organic substrates, which arises from the enzymatic pathways and substrates utilized.
 372 Lower ϵ values were consistently observed in deeper sediments compared to shallower layers.

373 Oxygen concentrations were measured across seven different profiles, and free O_2 was
 374 detectable only in the uppermost sediments, between 0.165 cm and 0.365 cm depth (Fig. 2P).
 375 Below 0.4 cm, sediments were consistently anoxic. The heterogeneous penetration of O_2 into
 376 the sediments is attributed to bioturbation, which was confirmed by visual observations of
 377 worm castings.

378

379 **3.3.4 Microbial community composition and chloroplast relative sequence abundances**

380 The microbial community in Lake Joux sediments was dominated by the phyla
 381 Chloroflexota, Nanoarchaeota, and Pseudomonadota (Fig. 3A). In the deep eutrophic
 382 sediments (below 30 cm), microbial species richness and evenness (Chao1 and Shannon alpha
 383 diversity indices) were significantly lower than in overlying layers (Fig. 3C). In this zone,
 384 Nanoarchaeota reached their highest relative sequence abundances ($>10\%$), decreasing to $\sim 7\%$
 385 in the shallower sediments. These elevated abundances, also reported in freshwater (Chen et
 386 al., 2023; Xie et al., 2024) and marine environments (Brick et al., 2025), likely reflect their
 387 wide environmental tolerance and host associations (Jarett et al., 2018) (Fig. 3A).

388 In the middle carbonate-rich interval (30–11 cm), microbial diversity increased, and
 389 Bacteroidota appeared, consistently representing $>5\%$ of the microbial community. Reduced
 390 relative abundances of chloroplast sequences in this layer (Fig. 3B) also indicate limited input
 391 from photosynthetic organisms during this depositional phase. Cyanobacteria-related ASVs
 392 displayed similar depth trends to chloroplast sequences, but with lower overall abundance,
 393 reaching a maximum of 2% at 4.5 cm depth (Fig. 3B). In the upper eutrophic sediments (11–0
 394 cm), Pseudomonadota became more abundant ($>20\%$) and chloroplast sequences markedly
 395 increased, reflecting enhanced sedimentation of photosynthetic organisms.



Microbial community composition was more similar within sedimentary intervals than between them (Fig. 3D). Stratification was especially pronounced for cyanobacterial and chloroplast sequences, which formed three distinct depth-specific clusters corresponding to the eutrophic, carbonate, and deep eutrophic intervals (Fig. S2). The methanotrophic community separated into two main groups, upper and deep eutrophic, while samples from the carbonate layer did not form a distinct cluster (Fig. S2). Methanogens, however, displayed clearer depth partitioning, with methylotrophic Methanomassiliicoccales dominating in the deep eutrophic interval and hydrogenotrophic Methanobacteriales increasing toward the surface (Fig. 4). Notably, depth patterns in methanogens and methanotrophs, as well as cyanobacterial and chloroplast-related sequences, tracked the same environmental gradients, with CH₄, NO₃⁻, and CRS showing the strongest correlations and AVS, δ¹³C_{org}, and sedimentary P as secondary correlates (Fig. 3E; Fig. S2).

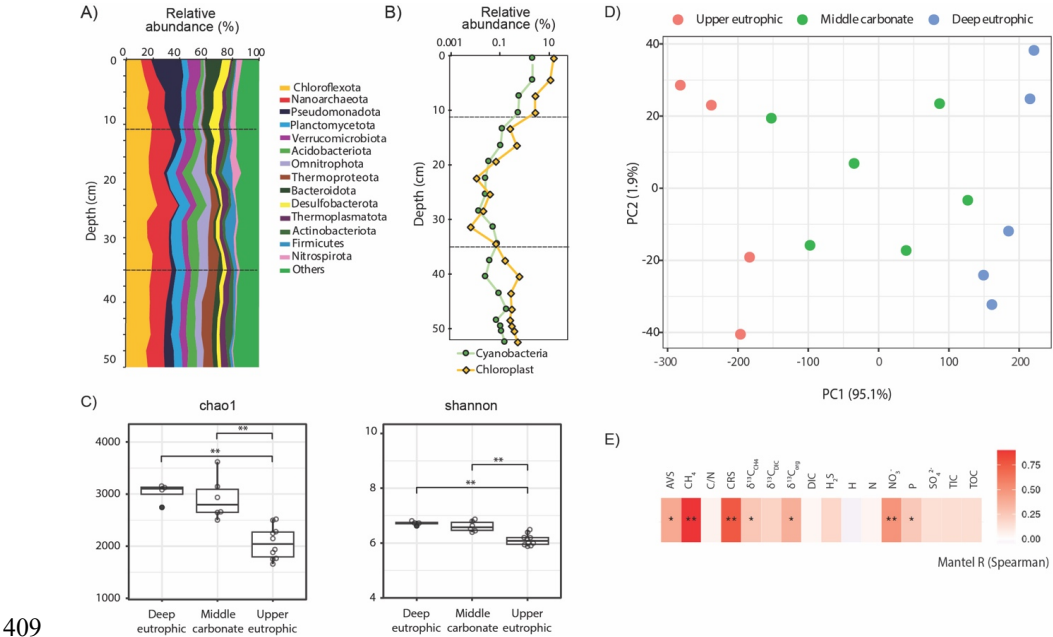


Figure 3 - (A) Relative 16S rRNA gene amplicon sequence abundances of bacterial and archaeal phyla, depicted as depth distribution in the 55 cm sedimentary profile of Lake Joux distribution; **(B)** Relative abundance of cyanobacteria and chloroplasts (algae and plants) affiliated 16S rRNA gene amplicon sequences in the 55 cm sedimentary profile of Lake Joux; **(C)** Alpha diversity (chao1 richness and Shannon diversity) of methanogens and methanotrophs. **(D)** Principal component ordination of centered log ratio (CLR) transformed 16S rRNA gene amplicon data, based on an Aitchison distance for which oversaturated distances were corrected and smoothed using LMdist. **(E)** Mantel tests results (Spearman's rank correlation) of community dissimilarity (corrected and smoothed Aitchison distance) and



environmental parameters (z-scored). P-values were adjusted for multiple testing using the false discovery rate (FDR) method. ** $p \leq 0.01$; * $p \leq 0.05$.

421

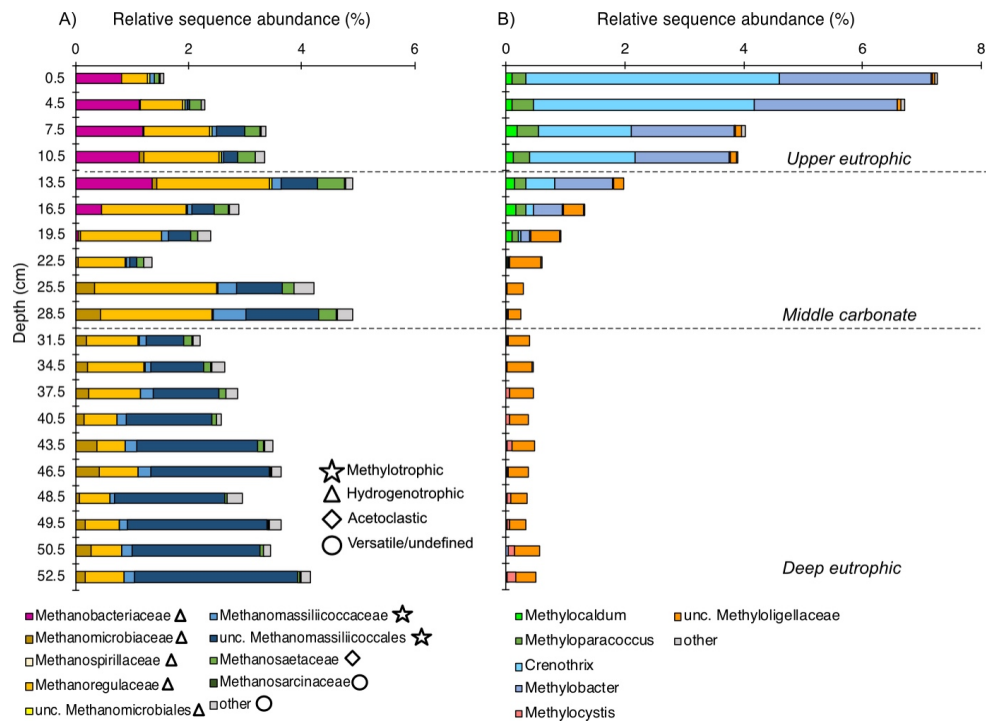
422 **3.3.4.1 Methanogenic and methanotrophic microbial communities**

423

424 The relative sequence abundance of archaeal methanogens consistently accounted for
 425 more than 1% of the microbial community across all sampled depths (Fig. 4A).
 426 Methanomassiliicoccales were the dominant methanogenic group in the deep eutrophic
 427 sediments, accounting for 1.4% of the microbial community at a depth of 37.5 cm (Fig. 4A).
 428 In contrast, Methanomicrobiales was the most abundant methanogen group in the middle
 429 carbonate interval, while Methanobacteriales sequences were most abundant in the upper
 430 eutrophic sediments (11–0 cm, Fig. 4A). Sequences affiliated with Methanosarcinales and
 431 Methyloacidiphilales were rare throughout the profile ($<0.01\%$).

432 In contrast, methanotrophic taxa were not correlated with sediment intervals but rather
 433 with dissolved P and N. In the deep and middle sediments below 19.5 cm, Rhizobiales-
 434 affiliated methylotrophs (e.g., Methylocystis, Methylocapsa, Methyloligellaceae, (Tamas et al.,
 435 2014; Vekeman et al., 2016) were the dominant putative methanotrophs, although they
 436 represented a modest portion of the community (max. 0.6%) (Fig. 4B). Anaerobic
 437 methanotrophs from ANME archaeal groups were not identified in the sedimentary profile of
 438 Lake Joux. Still, between 23 and 16 cm, Methyloirabilota NC10 bacteria capable of nitrite-
 439 dependent methane oxidation with intracellularly produced O_2 under anoxic conditions (Ettwig
 440 et al., 2010) were detected at a relative abundance of 0.2–1.3%.

441 The 16S rRNA gene sequences of aerobic MOBs represented between 0.3% and 8.7% of
 442 the microbial community throughout the sediment profile and were especially numerous ($>1\%$)
 443 above a depth of 19.5 cm (Fig. 3C). The most abundant methanotrophs from 19.5 cm depth to
 444 the surface were members of the order Methylococcales, mainly represented by two genera of
 445 MOB: *Crenothrix* and *Methylobacter* (Fig. 4B). At 0.5 cm depth, these two genera were
 446 notably abundant, accounting for 5% and 3% of 16S rRNA gene sequences, respectively (Fig.
 447 4).



448
449 **Figure 4** - Relative sequence abundance of (A) main methanogenic archaea taxa at family
450 taxonomic level and their pathways (B) and aerobic methanotrophic bacteria at genus
451 taxonomic level in the microbial community throughout 55 cm of the sedimentary profile of
452 Lake Joux.

453

454 4. Discussion

455 4.1 Tracing historical land use, industrialization, and eutrophication

456 The intensely black sediments abundant in chloroplast-related sequences and elevated TOC
457 content with low C:N ratios and light $\delta^{13}\text{C}_{\text{org}}$ in the deep eutrophic interval (55–30 cm, Fig. 1)
458 attest to a predominantly autochthonous organic matter, derived from phytoplankton blooms
459 (Lamb et al., 2006; Morales-Williams et al., 2017). Similar patterns recorded in other Lake
460 Joux sediment profiles (Dubois, 2016; Lavrieux et al., 2017; Magny et al., 2008) correspond to
461 a period of intensified deforestation and settlement expansion between 1525 and 1790 CE
462 (Dubois, 2016; Lavrieux et al., 2017; Magny et al., 2008). While no official records confirm
463 eutrophication during this period, these anthropogenic activities likely led to increased erosion
464 and sediment/nutrient transport, stimulating phytoplankton productivity (Fig. 1). Notably,
465 these sediments also exhibit high relative H_2S and AVS concentrations (Fig. 2B and 2K), which



466 are characteristic of late sediment diagenesis under eutrophic depositional conditions (Holmer
 467 and Storkholm, 2001).

468 The middle carbonate layer (30–11 cm depth) reflects a shift towards more oligotrophic
 469 conditions, likely linked to the abandonment of land-intensive activities and the switch to
 470 manufacturing in the 18th century. In addition, the 1777 construction of a dike between Lake
 471 Joux and Lake Brenet lowered the lake level by 3.6 m, mobilizing limestone-rich sediments
 472 (high TIC) and terrestrial plant material with heavier $\delta^{13}\text{C}_{\text{org}}$ and higher C/N ratios (Lavrieux
 473 et al., 2017; Magny et al., 2008; Monchamp et al., 2021) (Fig. 2). The sedimentological
 474 transition that marks the beginning of this interval at 30 cm depth aligns with a shift from
 475 methylophilic to hydrogenotrophic methanogens (Fig. 4), likely responsible for the lighter
 476 $\delta^{13}\text{C}_{\text{DIC}}$ values (Fig. 2F). Furthermore, the white-colored boundary of the middle carbonate
 477 layer (16–11 cm) coincides with warmer post-Little Ice Age conditions, promoting calcium
 478 carbonate precipitation and TIC enrichment (Lavrieux et al., 2017).

479 The upper eutrophic sedimentary interval (11–0 cm) consists of black sediments rich in
 480 TOC, lighter $\delta^{13}\text{C}_{\text{org}}$ values, low C/N ratios, and abundant chloroplast- and cyanobacteria-
 481 related sequences reflecting a well-documented 20th century eutrophication phase (Lavrieux et
 482 al., 2017; Magny et al., 2008; Monchamp et al., 2021) (Fig. 2, Fig. 3B). Elevated nutrient levels
 483 in this interval could result from external nutrient inputs trapped in porewater or from organic
 484 matter remineralization. Porewaters are strongly reducing, reflected by elevated H_2S and CRS,
 485 and the absence of O_2 below 0.5 cm. Upward diffusion of SO_4^{2-} meets downward-diffusing
 486 CH_4 , and in the 7.5–0 cm horizon, CH_4 concentrations fall sharply while $\delta^{13}\text{C}_{\text{CH}_4}$ becomes
 487 heavier and $\delta^{13}\text{C}_{\text{DIC}}$ lighter (Fig. 2A, B and K, M). Together with the dominance of MOB and
 488 the absence of ANME-related 16S rRNA gene amplicon sequences, these paired isotopic shifts
 489 indicate methanotrophy dominated by MOB as the main CH_4 sink in these anoxic, nutrient-
 490 replete surface sediments, whether sustained by micro-oxic niches or alternative oxidants (as
 491 discussed in further detail in 4.3).

492

493 **4.2 Methylophilic methanogens selected by past eutrophication**

494 Changes in organic matter sources to Lake Joux over the last four centuries appear
 495 closely tied to shifts in dominant methanogenic groups within its sediments. Deep eutrophic
 496 sediments, characterized by the highest CH_4 concentrations, are dominated by
 497 Methanomassiliicoccales, which are methanogens known to utilize methylated substrates such
 498 as dimethyl sulfide (DMS) and methylamines (Bueno De Mesquita et al., 2023; Ellenbogen et



al., 2024; Söllinger and Urich, 2019; Sun et al., 2019; Wang and Lee, 1994). The decomposition of algal and cyanobacterial biomass can release methylated sulfur compounds (including DMS and dimethylsulfoxide) and methylated amines, which stimulate methylotrophic methanogenesis in laboratory experiments and natural environments (Bose et al., 2008; Chistoserdova, 2011; Chistoserdova et al., 2009; Huang et al., 2018; Singh et al., 2005; Tebbe et al., 2023; Whiticar, 1999; Zhou et al., 2022).

Indirect evidence for the presence of methylated sulfur compounds comes from relatively higher concentrations of H_2S , AVS, and CRS at depth (Fig. 2B, 2K), indicating active sulfur cycling despite limited SO_4^{2-} availability. Furthermore, $\delta^{34}\text{S}$ values measured in CRS (primarily pyrite) consistently show positive isotopic signatures (7‰ to 10‰) in both the deep eutrophic and middle carbonate zones. While microbial SO_4^{2-} reduction typically produces ^{34}S -depleted sulfides ($\delta^{34}\text{S} < 0\text{‰}$) under open-system or moderately sulfate-limited conditions (Bradley et al., 2016; Canfield, 2001; Habicht and Canfield, 1997), the isotopic enrichment observed here is more consistent with either the degradation of sulfurized organic matter or methylated sulfur compounds (Phillips et al., 2022; Raven et al., 2019; Werne et al., 2004). These could simultaneously fuel methylotrophic methanogenesis and pyrite formation. This interpretation warrants confirmation through direct measurements of methylated sulfur species in future studies. Alternatively, the ^{34}S enrichment could reflect near complete consumption of a limited SO_4^{2-} pool so that ^{34}S sulfide reflects positive values of the original sulfate (Bernasconi et al., 2017)(Fig. 2).

Methylotrophic methanogenesis is typically a minor pathway in freshwater sediments because methylated substrates are scarce (Borrel et al., 2011; Bueno De Mesquita et al., 2023). However, in the deep eutrophic layer, prolonged algal biomass degradation likely generated a reservoir of recalcitrant methylated compounds (Achtnich et al., 1995; Rissanen et al., 2018), favoring methylotrophic methanogens. In contrast, hydrogenotrophic (using $\text{CO}_2 + \text{H}_2$) and acetoclastic (using acetate) methanogens primarily depend on fresh, labile organic matter, which rapidly becomes limited with burial (Achtnich et al., 1995; Meier et al., 2024; Rissanen et al., 2023; Rissanen et al., 2018). Thus, methylotrophs gain a selective advantage in these older, more refractory sediments. Above ~28.5 cm, as sediment inputs shift toward terrestrial organic matter and methylated substrate availability diminishes, methylotrophic methanogens decline and hydrogenotrophs progressively dominate (Fig. 4A).

To further support the interpretation of distinct methanogenic pathways, we analyzed the $\epsilon_{\text{Corg}-\text{CH}_4}$, reflecting the isotopic discrimination during CH_4 formation from C_{org} (Fig. 2O). We observed lower ϵ values in deeper eutrophic sediments compared to shallower zones.



Although interpreting specific metabolic pathways from isotopic fractionation is challenging in mixed microbial communities, the contrast in $\epsilon_{\text{Corg-CH}_4}$ (Fig. 2O) indicates distinct CH_4 -producing processes dominating at different sediment depths.

Our results support the view that eutrophication leaves a distinct imprint on methanogen stratification in sediments. In contrast to earlier studies that reported either weak vertical structuring (Meier et al., 2024) or only subtle shifts in methanogen dominance (Rissanen et al., 2023), we found clear zonation with Methanomassiliicoccales prevailing in the deepest eutrophic interval, Methanomicrobiaceae in the carbonate-rich middle section, and Methanobacteriaceae dominating the upper eutrophic sediments. Considered alongside these previous observations in other lakes, our findings question the usefulness of broad generalizations and suggest that methanogen communities are primarily shaped by habitat-specific conditions—such as lithology, organic-matter quality, and redox context—rather than exhibiting universal hydrogenotroph dominance. By comparison, a pronounced vertical structuring of methane-oxidizing bacteria appears more consistent across systems (Mayr et al., 2020; Rissanen et al., 2018; Van Grinsven et al., 2022).

4.3 Aerobic methanotrophs are selected by nutrient availability

Within sediments, CH_4 is typically oxidized anaerobically (Borrel et al., 2011; Martinez-Cruz et al., 2018). Interestingly, in the anoxic sediments of Lake Joux, anaerobic methanotrophic archaea are not detectable. Sequences related to *Candidatus Methyloirabilis*—capable of intracellular O_2 production to fuel methane monooxygenase activity—occur in notable relative sequence abundances but are confined to 16–23 cm depth within the middle carbonate interval, but are relatively scarce compared to their aerobic counterparts. Namely, gammaproteobacterial MOB 16S rRNA gene sequences recovered from Lake Joux sediments are highly abundant (1–9%) from 19.5 cm upward, despite prevailing anoxic conditions (Fig. 4, 5). The MOB 16S rRNA gene sequences primarily affiliate with Methylococcales, notably the genera *Crenothrix* and *Methylobacter* (Fig. 5). The dominance of Methylococcales associated MOB in the methane-oxidation zone suggests that serve as the dominant CH_4 sink in these nutrient-replete but anoxic surface sediments (Fig. 2N, Fig. 5).

How these aerobic methanotrophs meet their O_2 demand below 0.4 cm—where no O_2 could be detected, remains unresolved. Nanomolar O_2 cannot be excluded, but diffusive supply from the sediment–water interface to higher sediment depths is implausible. While some Methylococcales respire alternative electron acceptors (e.g., nitrate, Fe(III)) at low O_2 levels (Li et al., 2023; Van Grinsven et al., 2020; Yang et al., 2025), methane monooxygenase remains



567 O₂-dependent for the oxidation of CH₄ to methanol. Three microbial mechanisms could
 568 generate microscale O₂ at depth within the sediment ("dark O₂"): methanobactin-mediated
 569 water splitting (Dershwitz et al., 2021), chlorite (ClO₂⁻) dismutation by (per)chlorate-respiring
 570 bacteria (Xu and Logan, 2003), and nitric-oxide dismutation as described for NC10 bacteria
 571 (Ettwig et al., 2010).

572 Water lysis appears energetically unfavorable in natural systems and is associated with
 573 Alphaproteobacterial methanotrophs, which are not prevalent in Lake Joux (Dershwitz et al.,
 574 2021). Chlorite dismutation, catalyzed by chlorite dismutase found in over 60 genera across 13
 575 phyla (Barnum and Coates, 2023), could be a source of O₂, as Pseudomonadota and
 576 Actinobacteria are abundant in these sediments (Fig. 3A). However, environmental levels of
 577 (per)chlorate are likely too low to support this pathway at significant levels (Lv et al., 2019;
 578 Miller et al., 2014; Wang et al., 2024).

579 A more plausible mechanism is NO dismutation via the nitric oxide dismutase (NOD)
 580 enzyme, which has been recently attributed to several families within the phylum Bacteroidota
 581 (Ruff et al., 2024). In Lake Joux, putatively NOD-containing Bacteroidota account for $\sim 0.54 \pm$
 582 0.2% of the microbial community in the upper eutrophic sediments, suggesting this pathway
 583 may contribute to localized O₂ production. Notably, while gammaproteobacterial
 584 methanotrophs, including *Crenothrix* and *Methylobacter*, possess genes for respiratory NO₃⁻
 585 reduction (Almog et al., 2024; He et al., 2022; Martinez-Cruz et al., 2017; Milucka et al., 2012;
 586 Schorn et al., 2024), active NO₃⁻ respiration has only been demonstrated experimentally for
 587 *Methylomonas denitrificans* cultures (Kits et al., 2015) and indirectly by denitrification gene
 588 expression by MOB in Lake Zug (Schorn et al., 2024). The latter study revealed that *Crenothrix*
 589 and *Methylobacter* related microorganisms continue CH₄ oxidation in hypoxic and anoxic
 590 regions of the water column by performing denitrification or fermentation-based
 591 methanotrophy (Schorn et al., 2024). In Lake Joux, these same MOB taxa dominate the highly
 592 reducing, upper eutrophic sediments (Fig. 4B).

593 Interestingly, we observed strong positive correlations ($p < 0.05$) between the relative
 594 sequence abundances of *Crenothrix* and *Methylobacter* and porewater NO₃⁻ and PO₄³⁻ (Fig. 5).
 595 These nutrients exhibited moderate correlation with each other ($R^2 = 0.72$). While the source
 596 of NO₃⁻ cannot be resolved here, possible mechanisms of NO₃⁻ generation include oxidation of
 597 NH₄⁺ by Mn(IV) or Fe(III) oxides. Importantly, the MOB–nutrient correlations may also reflect
 598 a shared response to favorable near-surface conditions (e.g., sustained inputs of labile organic
 599 matter or higher porosity), rather than direct nutrient control. Nevertheless, it has been
 600 experimentally demonstrated that PO₄³⁻, NO₃⁻, and NH₄⁺ additions can directly enhance CH₄



oxidation rates by MOB and, in particular, *Methylobacter* (Almog et al., 2024; Kits et al., 2015; Nijman et al., 2022; Xia et al., 2021; Yang et al., 2025). Taken together, these observations suggest that nutrient availability may play a direct role in shaping the structure and activity of MOB communities.

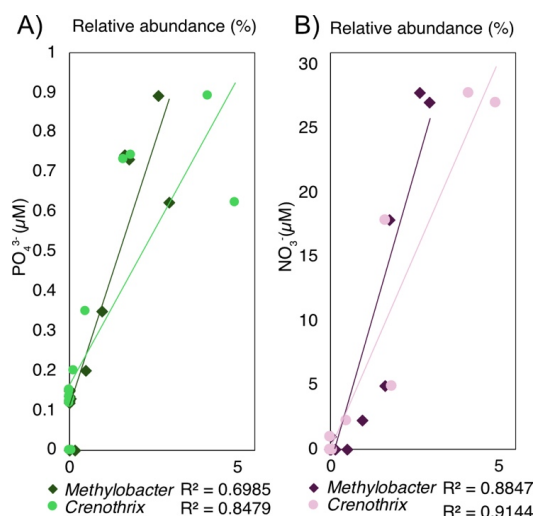


Figure 5 - (A) Correlation between PO_4^{3-} concentration and the relative sequence abundance of *Crenothrix* and *Methylobacter*. **(B)** Correlation between NO_3^- concentration and the relative sequence abundance of *Crenothrix* and *Methylobacter*.

5. Conclusion

Our results show that historical eutrophication left a lasting sedimentary legacy that structures contemporary methane-cycling microbial communities, selecting methylotrophic methanogens. In upper eutrophic, anoxic sediments, the surprisingly high relative sequence abundances of MOB (up to ~9%) specifically Methylococcales-affiliated Gammaproteobacteria, co-vary with elevated NO_3^- and PO_4^{3-} concentrations. This suggests that eutrophication can simultaneously stimulate CH_4 production and enhance its oxidation by shaping microbial assemblages.

As eutrophication continues to alter freshwater systems globally, understanding nutrient- and substrate-driven shifts in CH_4 -cycling communities becomes increasingly important. Future studies should focus on elucidating the in situ activity of aerobic methanotrophs and molecular mechanism of methane oxidation under anoxic conditions, as presumably aerobic MOB have been widely reported in anoxic sediments (Almog et al., 2024; Ruff et al., 2024; Schorn et al., 2024). Combining molecular, isotopic, and geochemical



624 approaches will be essential to better constrain methane fluxes in lakes undergoing or
 625 recovering from eutrophication.

626

627 **Data availability**

628 All geochemical data are included in this published article and its supplementary information
 629 files. The 16S rRNA gene amplicon sequencing data has been deposited at the Sequence Read
 630 Archive under the BioProject accession PRJNA1207472.

631

632 **Author contribution**

633 ABS contributed to conceptualization, data curation, formal analysis, funding acquisition,
 634 methodology, supervision, validation, visualization, writing original draft preparation, review,
 635 and editing. ERBB contributed to data curation, formal analysis, and manuscript editing; SK
 636 contributed to data curation, formal analysis, and manuscript editing; MEM contributed to
 637 resources and manuscript editing; JS contributed to data curation, formal analysis,
 638 methodology, validation, visualization, designing and implementing computer codes, and
 639 writing original draft preparation, review, and editing. PP contributed to conceptualization,
 640 formal analysis, funding acquisition, supervision, validation, visualization, writing original
 641 draft preparation, review, and editing. JSB contributed to conceptualization, formal analysis,
 642 funding acquisition, supervision, validation, visualization, writing original draft preparation,
 643 review, and editing.

644

645 **Competing interests**

646 The authors declare that they have no conflict of interest.

647

648 **Acknowledgments**

649 The authors would like to extend their gratitude to Floreana Marie Miesen (UNIL) for her
 650 invaluable support with fieldwork and logistics; to Dr. Carsten Schubert (EAWAG) for
 651 providing access to laboratory facilities for methane analyses; to Dr. Giulia Ceriotti (UNIL) for
 652 analytical and logistical support with methane analyses; to Laetitia Monbaron and Micaela
 653 Faria (UNIL) for their technical assistance in the laboratory; to Jorge Spangenberg (UNIL) for
 654 his support in methodology development and analytical assistance; to Frédéric Lardet for
 655 assistance with Fig. 1; and to Dr. William Leavitt (The University of Utah) for his help during
 656 fieldwork. Special thanks are also due to the Fondation Agassiz for the individual grant



awarded to the first author, ABS, which made this study possible. The amplicon sequencing section of this work has been achieved using the Life Science Compute Cluster (LiSC) of the University of Vienna.

Financial Support

This study was funded by the 2022 Fondation Agassiz awarded to ABS.

References

- Achtnich, C., Bak, F., and Conrad, R.: Competition for electron donors among nitrate reducers, ferric iron reducers, sulfate reducers, and methanogens in anoxic paddy soil, *Biology and fertility of soils*, 19, 65-72, 1995.
- Almog, G., Rubin-Blum, M., Murrell, J. C., Vigderovich, H., Eckert, W., Larke-Mejía, N., and Sivan, O.: Survival strategies of aerobic methanotrophs to hypoxia in methanogenic lake sediments, 2024.
- Apprill, A., McNally, S., Parsons, R., and Weber, L.: Minor revision to V4 region SSU rRNA 806R gene primer greatly increases detection of SAR11 bacterioplankton, *Aquatic Microbial Ecology*, 75, 129-137, 2015.
- Barker, J. F. and Fritz, P.: Carbon isotope fractionation during microbial methane oxidation, *Nature*, 293, 289-291, 1981.
- Barnett, D. J., Arts, I. C., and Penders, J.: microViz: an R package for microbiome data visualization and statistics, *Journal of Open Source Software*, 6, 3201, 2021.
- Barnum, T. P. and Coates, J. D.: Chlorine redox chemistry is widespread in microbiology, *The ISME journal*, 17, 70-83, 2023.
- Bastviken, D., Cole, J., Pace, M., and Tranvik, L.: Methane emissions from lakes: Dependence of lake characteristics, two regional assessments, and a global estimate, *Global biogeochemical cycles*, 18, 2004.
- Bastviken, D., Cole, J. J., Pace, M. L., and Van de Bogert, M. C.: Fates of methane from different lake habitats: Connecting whole-lake budgets and CH₄ emissions, *Journal of Geophysical Research: Biogeosciences*, 113, 2008.
- Bastviken, D., Tranvik, L. J., Downing, J. A., Crill, P. M., and Enrich-Prast, A.: Freshwater methane emissions offset the continental carbon sink, *Science*, 331, 50-50, 2011.
- Beaulieu, J. J., DelSontro, T., and Downing, J. A.: Eutrophication will increase methane emissions from lakes and impoundments during the 21st century, *Nature communications*, 10, 1375, 2019.
- Bernasconi, S. M., Meier, I., Wohlgend, S., Brack, P., Hochuli, P. A., Bläsi, H., Wortmann, U. G., and Ramseyer, K.: An evaporite-based high-resolution sulfur isotope record of Late Permian and Triassic seawater sulfate, *Geochimica et Cosmochimica Acta*, 204, 331-349, 2017.
- Blaser, M. and Conrad, R.: Stable carbon isotope fractionation as tracer of carbon cycling in anoxic soil ecosystems, *Current opinion in biotechnology*, 41, 122-129, 2016.
- Borrel, G., Jézéquel, D., Biderre-Petit, C., Morel-Desrosiers, N., Morel, J.-P., Peyret, P., Fonty, G., and Lehours, A.-C.: Production and consumption of methane in freshwater lake ecosystems, *Research in microbiology*, 162, 832-847, 2011.
- Bose, A., Pritchett, M. A., and Metcalf, W. W.: Genetic analysis of the methanol- and methylamine-specific methyltransferase 2 genes of *Methanosarcina acetivorans* C2A, *Journal of bacteriology*, 190, 4017-4026, 2008.



- 703 Bradley, A., Leavitt, W., Schmidt, M., Knoll, A. H., Girguis, P. R., and Johnston, D. T.:
704 Patterns of sulfur isotope fractionation during microbial sulfate reduction, *Geobiology*, 14, 91-
705 101, 2016.
- 706 Brick, S., Niggemann, J., Reckhardt, A., Könneke, M., and Engelen, B.: Interstitial microbial
707 communities of coastal sediments are dominated by Nanoarchaeota, *Frontiers in Microbiology*,
708 16, 1532193, 2025.
- 709 Bueno de Mesquita, C. P., Wu, D., and Tringe, S. G.: Methyl-based methanogenesis: an
710 ecological and genomic review, *Microbiology and Molecular Biology Reviews*, 87, e00024-
711 00022, 2023.
- 712 Callahan, B. J., Sankaran, K., Fukuyama, J. A., McMurdie, P. J., and Holmes, S. P.:
713 Bioconductor workflow for microbiome data analysis: from raw reads to community analyses,
714 *F1000Research*, 5, 2016a.
- 715 Callahan, B. J., McMurdie, P. J., Rosen, M. J., Han, A. W., Johnson, A. J. A., and Holmes, S.
716 P.: DADA2: High-resolution sample inference from Illumina amplicon data, *Nature methods*,
717 13, 581-583, 2016b.
- 718 Canfield, D. E.: Isotope fractionation by natural populations of sulfate-reducing bacteria,
719 *Geochimica et Cosmochimica Acta*, 65, 1117-1124, 2001.
- 720 Chen, M., Conroy, J. L., Sanford, R. A., Wyman-Feravich, D. A., Chee-Sanford, J. C., and
721 Connor, L. M.: Tropical lacustrine sediment microbial community response to an extreme El
722 Niño event, *Scientific reports*, 13, 6868, 2023.
- 723 Chistoserdova, L.: Modularity of methylotrophy, revisited, *Environmental microbiology*, 13,
724 2603-2622, 2011.
- 725 Chistoserdova, L., Kalyuzhnaya, M. G., and Lidstrom, M. E.: The expanding world of
726 methylotrophic metabolism, *Annual review of microbiology*, 63, 477-499, 2009.
- 727 Cline, J. D.: Spectrophotometric determination of hydrogen sulfide in natural waters,
728 *Limnology and Oceanography*, 14, 454-458, 1969.
- 729 Conrad, R.: Quantification of methanogenic pathways using stable carbon isotopic signatures:
730 a review and a proposal, *Organic geochemistry*, 36, 739-752, 2005.
- 731 Conrad, R.: Microbial ecology of methanogens and methanotrophs, *Advances in agronomy*,
732 96, 1-63, 2007.
- 733 Conrad, R.: Importance of hydrogenotrophic, acetoclastic and methylotrophic methanogenesis
734 for methane production in terrestrial, aquatic and other anoxic environments: a mini review,
735 *Pedosphere*, 30, 25-39, 2020.
- 736 Dean, J. F., Middelburg, J. J., Röckmann, T., Aerts, R., Blauw, L. G., Egger, M., Jetten, M. S.,
737 de Jong, A. E., Meisel, O. H., and Rasigraf, O.: Methane feedbacks to the global climate system
738 in a warmer world, *Reviews of Geophysics*, 56, 207-250, 2018.
- 739 Dershwitz, P., Bandow, N. L., Yang, J., Semrau, J. D., McEllistrem, M. T., Heinze, R. A.,
740 Fonseca, M., Ledesma, J. C., Jennett, J. R., and DiSpirito, A. M.: Oxygen generation via water
741 splitting by a novel biogenic metal ion-binding compound, *Applied and Environmental*
742 *Microbiology*, 87, e00286-00221, 2021.
- 743 Deutzmann, J. S. and Schink, B.: Anaerobic oxidation of methane in sediments of Lake
744 Constance, an oligotrophic freshwater lake, *Applied and environmental microbiology*, 77,
745 4429-4436, 2011.
- 746 Dubois, N.: Traces of history in the sediments of Lake Joux, 2016.
- 747 Ellenbogen, J. B., Borton, M. A., McGivern, B. B., Cronin, D. R., Hoyt, D. W., Freire-Zapata,
748 V., McCalley, C. K., Varner, R. K., Crill, P. M., and Wehr, R. A.: Methylotrophy in the Mire:
749 direct and indirect routes for methane production in thawing permafrost, *Msystems*, 9, e00698-
750 00623, 2024.



- 751 Ettwig, K. F., Butler, M. K., Le Paslier, D., Pelletier, E., Mangenot, S., Kuypers, M. M.,
752 Schreiber, F., Dutilh, B. E., Zedelius, J., and de Beer, D.: Nitrite-driven anaerobic methane
753 oxidation by oxygenic bacteria, *Nature*, 464, 543-548, 2010.
- 754 Fiskal, A., Deng, L., Michel, A., Eickenbusch, P., Han, X., Lagostina, L., Zhu, R., Sander, M.,
755 Schroth, M. H., and Bernasconi, S. M.: Effects of eutrophication on sedimentary organic
756 carbon cycling in five temperate lakes, *Biogeosciences*, 16, 3725-3746, 2019.
- 757 Garcia, J.-L., Patel, B. K., and Ollivier, B.: Taxonomic, phylogenetic, and ecological diversity
758 of methanogenic Archaea, *Anaerobe*, 6, 205-226, 2000.
- 759 Habicht, K. S. and Canfield, D. E.: Sulfur isotope fractionation during bacterial sulfate
760 reduction in organic-rich sediments, *Geochimica et Cosmochimica Acta*, 61, 5351-5361, 1997.
- 761 Han, X.: Influence of eutrophication on microbial community structure, organic carbon
762 sources, and organic carbon degradation in lake sediments through time, ETH Zurich, 2020.
- 763 Hanson, R. S. and Hanson, T. E.: Methanotrophic bacteria, *Microbiological reviews*, 60, 439-
764 471, 1996.
- 765 He, R., Wang, J., Pohlman, J. W., Jia, Z., Chu, Y.-X., Wooller, M. J., and Leigh, M. B.:
766 Metabolic flexibility of aerobic methanotrophs under anoxic conditions in Arctic lake
767 sediments, *The ISME Journal*, 16, 78-90, 2022.
- 768 Ho, A., Kerckhof, F. M., Luke, C., Reim, A., Krause, S., Boon, N., and Bodelier, P. L.:
769 Conceptualizing functional traits and ecological characteristics of methane-oxidizing bacteria
770 as life strategies, *Environmental Microbiology Reports*, 5, 335-345, 2013.
- 771 Holmer, M. and Storkholm, P.: Sulphate reduction and sulphur cycling in lake sediments: a
772 review, *Freshwater Biology*, 46, 431-451, 2001.
- 773 Hoops, S. L. and Knights, D.: LMDist: Local Manifold distance accurately measures beta
774 diversity in ecological gradients, *Bioinformatics*, 39, btad727, 2023.
- 775 Huang, H., Xu, X., Shi, C., Liu, X., and Wang, G.: Response of taste and odor compounds to
776 elevated cyanobacteria biomass and temperature, *Bulletin of environmental contamination and
777 toxicology*, 101, 272-278, 2018.
- 778 Huang, R., Soneson, C., Ernst, F. G., Rue-Albrecht, K. C., Yu, G., Hicks, S. C., and Robinson,
779 M. D.: TreeSummarizedExperiment: a S4 class for data with hierarchical structure,
780 *F1000Research*, 9, 1246, 2021.
- 781 Jahnke, L. L., Summons, R. E., Hope, J. M., and Des Marais, D. J.: Carbon isotopic
782 fractionation in lipids from methanotrophic bacteria II: The effects of physiology and
783 environmental parameters on the biosynthesis and isotopic signatures of biomarkers,
784 *Geochimica et Cosmochimica Acta*, 63, 79-93, 1999.
- 785 Jarett, J. K., Nayfach, S., Podar, M., Inskeep, W., Ivanova, N. N., Munson-McGee, J., Schulz,
786 F., Young, M., Jay, Z. J., and Beam, J. P.: Single-cell genomics of co-sorted Nanoarchaeota
787 suggests novel putative host associations and diversification of proteins involved in symbiosis,
788 *Microbiome*, 6, 1-14, 2018.
- 789 Jørgensen, B. B., Weber, A., and Zopf, J.: Sulfate reduction and anaerobic methane oxidation
790 in Black Sea sediments, *Deep Sea Research Part I: Oceanographic Research Papers*, 48, 2097-
791 2120, 2001.
- 792 Kits, K. D., Klotz, M. G., and Stein, L. Y.: Methane oxidation coupled to nitrate reduction
793 under hypoxia by the Gammaproteobacterium *Methylomonas denitrificans*, *sp. nov.* type strain
794 FJG1, *Environmental microbiology*, 17, 3219-3232, 2015.
- 795 Knief, C.: Diversity and habitat preferences of cultivated and uncultivated aerobic
796 methanotrophic bacteria evaluated based on *pmoA* as molecular marker, *Frontiers in
797 microbiology*, 6, 1346, 2015.
- 798 Knittel, K. and Boetius, A.: Anaerobic oxidation of methane: progress with an unknown
799 process, *Annual review of microbiology*, 63, 311-334, 2009.



- 800 Lamb, A. L., Wilson, G. P., and Leng, M. J.: A review of coastal palaeoclimate and relative
801 sea-level reconstructions using $\delta^{13}\text{C}$ and C/N ratios in organic material, *Earth-Science*
802 *Reviews*, 75, 29-57, 2006.
- 803 Lavrieux, M., Schubert, C. J., Hofstetter, T., Eglinton, T. I., Hajdas, I., Wacker, L., and Dubois,
804 N.: From medieval land clearing to industrial development: 800 years of human-impact history
805 in the Joux Valley (Swiss Jura), *The Holocene*, 27, 1443-1454, 2017.
- 806 Li, B., Tao, Y., Mao, Z., Gu, Q., Han, Y., Hu, B., Wang, H., Lai, A., Xing, P., and Wu, Q. L.:
807 Iron oxides act as an alternative electron acceptor for aerobic methanotrophs in anoxic lake
808 sediments, *Water Research*, 234, 119833, 2023.
- 809 Lods-Crozet, B., Reymond, O., and Strawczynski, A.: Evaluation de la qualité chimique et
810 biologique du lac de Joux (Jura Suisse) entre 1985 et 2004, *Bull Soc Ne Sci Nat*, 129, 29-47,
811 2006.
- 812 Lv, P.-L., Shi, L.-D., Wang, Z., Rittmann, B., and Zhao, H.-P.: Methane oxidation coupled to
813 perchlorate reduction in a membrane biofilm batch reactor, *Science of the Total Environment*,
814 667, 9-15, 2019.
- 815 Magny, M., Gauthier, E., Vannière, B., and Peyron, O.: Palaeohydrological changes and
816 human-impact history over the last millennium recorded at Lake Joux in the Jura Mountains,
817 Switzerland, *The Holocene*, 18, 255-265, 2008.
- 818 Martinez-Cruz, K., Sepulveda-Jauregui, A., Casper, P., Anthony, K. W., Smemo, K. A., and
819 Thalasso, F.: Ubiquitous and significant anaerobic oxidation of methane in freshwater lake
820 sediments, *Water Research*, 144, 332-340, 2018.
- 821 Martinez-Cruz, K., Leewis, M.-C., Herriott, I. C., Sepulveda-Jauregui, A., Anthony, K. W.,
822 Thalasso, F., and Leigh, M. B.: Anaerobic oxidation of methane by aerobic methanotrophs in
823 sub-Arctic lake sediments, *Science of the Total Environment*, 607, 23-31, 2017.
- 824 Mayr, M. J., Zimmermann, M., Guggenheim, C., Brand, A., and Bürgmann, H.: Niche
825 partitioning of methane-oxidizing bacteria along the oxygen-methane counter gradient of
826 stratified lakes, *The ISME journal*, 14, 274-287, 2020.
- 827 McLaren, M. R. and Callahan, B. J.: Silva 138.1 prokaryotic SSU taxonomic training data
828 formatted for DADA2, Zenodo, 2021.
- 829 McMurdie, P. J. and Holmes, S.: phyloseq: an R package for reproducible interactive analysis
830 and graphics of microbiome census data, *PloS one*, 8, e61217, 2013.
- 831 Meier, D., van Grinsven, S., Michel, A., Eickenbusch, P., Glombitza, C., Han, X., Fiskal, A.,
832 Bernasconi, S., Schubert, C. J., and Lever, M. A.: Hydrogen-independent CO_2 reduction
833 dominates methanogenesis in five temperate lakes that differ in trophic states, *ISME*
834 *Communications*, ycae089, 2024.
- 835 Meyers, P. A.: Preservation of elemental and isotopic source identification of sedimentary
836 organic matter, *Chemical geology*, 114, 289-302, 1994.
- 837 Miller, L. G., Baesman, S. M., Carlström, C. I., Coates, J. D., and Oremland, R. S.: Methane
838 oxidation linked to chlorite dismutation, *Frontiers in Microbiology*, 5, 275, 2014.
- 839 Milucka, J., Ferdelman, T. G., Polerecky, L., Franzke, D., Wegener, G., Schmid, M.,
840 Lieberwirth, I., Wagner, M., Widdel, F., and Kuypers, M. M.: Zero-valent sulphur is a key
841 intermediate in marine methane oxidation, *Nature*, 491, 541-546, 2012.
- 842 Mitchell, E., van der Knaap, W. O., van Leeuwen, J. F., Buttler, A., Warner, B. G., and Gobat,
843 J.-M.: The palaeoecological history of the Praz-Rodet bog (Swiss Jura) based on pollen, plant
844 macrofossils and testate amoebae (Protozoa), *The Holocene*, 11, 65-80, 2001.
- 845 Monchamp, M.-É., Bruel, R., Frossard, V., McGowan, S., Lavrieux, M., Muschick, M., Perga,
846 M.-É., and Dubois, N.: Paleoecological evidence for a multi-trophic regime shift in a perialpine
847 lake (Lake Joux, Switzerland), *Anthropocene*, 35, 100301, 2021.



- 848 Morales-Williams, A. M., Wanamaker Jr, A. D., and Downing, J. A.: Cyanobacterial carbon
 849 concentrating mechanisms facilitate sustained CO₂ depletion in eutrophic lakes,
 850 *Biogeosciences*, 14, 2865-2875, 2017.
- 851 Nijman, T. P., Amado, A. M., Bodelier, P. L., and Veraart, A. J.: Relief of phosphate limitation
 852 stimulates methane oxidation, *Frontiers in Environmental Science*, 10, 804512, 2022.
- 853 Oswald, K., Milucka, J., Brand, A., Hach, P., Littmann, S., Wehrli, B., Kuypers, M. M., and
 854 Schubert, C. J.: Aerobic gammaproteobacterial methanotrophs mitigate methane emissions
 855 from oxic and anoxic lake waters, *Limnology and Oceanography*, 61, S101-S118, 2016.
- 856 Parada, A. E., Needham, D. M., and Fuhrman, J. A.: Every base matters: assessing small
 857 subunit rRNA primers for marine microbiomes with mock communities, time series and global
 858 field samples, *Environmental microbiology*, 18, 1403-1414, 2016.
- 859 Penger, J., Conrad, R., and Blaser, M.: Stable carbon isotope fractionation by methylotrophic
 860 methanogenic archaea, *Applied and environmental microbiology*, 78, 7596-7602, 2012.
- 861 Phillips, A. A., White, M. E., Seidel, M., Wu, F., Pavia, F. F., Kemeny, P. C., Ma, A. C.,
 862 Aluwihare, L. I., Dittmar, T., and Sessions, A. L.: Novel sulfur isotope analyses constrain
 863 sulfurized porewater fluxes as a minor component of marine dissolved organic matter,
 864 *Proceedings of the National Academy of Sciences*, 119, e2209152119, 2022.
- 865 Pigué, A.: Le territoire et la commune du Lieu jusqu'en 1536, 1946.
- 866 Pjevac, P., Hausmann, B., Schwarz, J., Kohl, G., Herbold, C. W., Loy, A., and Berry, D.: An
 867 economical and flexible dual barcoding, two-step PCR approach for highly multiplexed
 868 amplicon sequencing, *Frontiers in microbiology*, 12, 669776, 2021.
- 869 Quast, C., Pruesse, E., Yilmaz, P., Gerken, J., Schweer, T., Yarza, P., Peplies, J., and Glöckner,
 870 F. O.: The SILVA ribosomal RNA gene database project: improved data processing and web-
 871 based tools, *Nucleic acids research*, 41, D590-D596, 2012.
- 872 Raven, M., Fike, D., Gomes, M., and Webb, S.: Chemical and isotopic evidence for organic
 873 matter sulfurization in redox gradients around mangrove roots, *Frontiers in Earth Science*, 7,
 874 98, 2019.
- 875 Reis, P. C., Thottathil, S. D., Ruiz-González, C., and Prairie, Y. T.: Niche separation within
 876 aerobic methanotrophic bacteria across lakes and its link to methane oxidation rates,
 877 *Environmental microbiology*, 22, 738-751, 2020.
- 878 Reis, P. C., Tsuji, J. M., Weiblen, C., Schiff, S. L., Scott, M., Stein, L. Y., and Neufeld, J. D.:
 879 Enigmatic persistence of aerobic methanotrophs in oxygen-limiting freshwater habitats, *The*
 880 *ISME Journal*, 18, wræ041, 2024.
- 881 Rissanen, A. J., Saarenheimo, J., Tirola, M., Peura, S., Aalto, S. L., Karvinen, A., and
 882 Nykänen, H.: Gammaproteobacterial methanotrophs dominate methanotrophy in aerobic and
 883 anaerobic layers of boreal lake waters, *Aquatic Microbial Ecology*, 81, 257-276, 2018.
- 884 Rissanen, A. J., Jilbert, T., Simojoki, A., Mangayil, R., Aalto, S. L., Khanongnuch, R., Peura,
 885 S., and Jäntti, H.: Organic matter lability modifies the vertical structure of methane-related
 886 microbial communities in lake sediments, *Microbiology spectrum*, 11, e01955-01923, 2023.
- 887 Ruff, S. E., Schwab, L., Vidal, E., Hemingway, J. D., Kraft, B., and Murali, R.: Widespread
 888 occurrence of dissolved oxygen anomalies, aerobic microbes, and oxygen-producing metabolic
 889 pathways in apparently anoxic environments, *FEMS Microbiology Ecology*, 100, fiae132,
 890 2024.
- 891 Sanches, L. F., Guenet, B., Marinho, C. C., Barros, N., and de Assis Esteves, F.: Global
 892 regulation of methane emission from natural lakes, *Scientific Reports*, 9, 255, 2019.
- 893 Saunois, M., Stavert, A., Poulter, B., Bousquet, P., Canadell, J., Jackson, R., Raymond, P.,
 894 Dlugokencky, E., Houweling, S., and Patra, P.: The Global Methane Budget 2000–2017, *Earth*
 895 *Syst. Sci. Data*, 12, 1561–1623, 2020.



- 896 Schorn, S., Graf, J. S., Littmann, S., Hach, P. F., Lavik, G., Speth, D. R., Schubert, C. J.,
 897 Kuypers, M. M., and Milucka, J.: Persistent activity of aerobic methane-oxidizing bacteria in
 898 anoxic lake waters due to metabolic versatility, *Nature Communications*, 15, 5293, 2024.
 899 Singh, N., Kendall, M. M., Liu, Y., and Boone, D. R.: Isolation and characterization of
 900 methylophilic methanogens from anoxic marine sediments in Skan Bay, Alaska: description
 901 of *Methanococcoides alaskense* sp. nov., and emended description of *Methanosarcina baltica*,
 902 *International journal of systematic and evolutionary microbiology*, 55, 2531-2538, 2005.
 903 Söllinger, A. and Urich, T.: Methylophilic methanogens everywhere—physiology and
 904 ecology of novel players in global methane cycling, *Biochemical Society Transactions*, 47,
 905 1895-1907, 2019.
 906 Spangenberg, J. E. and Bosco-Santos, A.: Sulfur isotope analyses using $3\times$ elemental
 907 analysis/isotope ratio mass spectrometry: Saving helium and energy while reducing analytical
 908 time and costs, *Rapid Communications in Mass Spectrometry*, 38, e9866, 2024.
 909 Sun, J., Mausz, M. A., Chen, Y., and Giovannoni, S. J.: Microbial trimethylamine metabolism
 910 in marine environments, *Environmental Microbiology*, 21, 513-520, 2019.
 911 Tamas, I., Smirnova, A. V., He, Z., and Dunfield, P. F.: The (d) evolution of methanotrophy in
 912 the Beijerinckiaceae—a comparative genomics analysis, *The ISME journal*, 8, 369-382, 2014.
 913 Tebbe, D. A., Gruender, C., Dlugosch, L., Löhmus, K., Rolfes, S., Könneke, M., Chen, Y.,
 914 Engelen, B., and Schäfer, H.: Microbial drivers of DMSO reduction and DMS-dependent
 915 methanogenesis in saltmarsh sediments, *The ISME Journal*, 17, 2340-2351, 2023.
 916 Templeton, A. S., Chu, K.-H., Alvarez-Cohen, L., and Conrad, M. E.: Variable carbon isotope
 917 fractionation expressed by aerobic CH_4 -oxidizing bacteria, *Geochimica et Cosmochimica*
 918 *Acta*, 70, 1739-1752, 2006.
 919 Tranvik, L. J., Downing, J. A., Cotner, J. B., Loiselle, S. A., Striegl, R. G., Ballatore, T. J.,
 920 Dillon, P., Finlay, K., Fortino, K., and Knoll, L. B.: Lakes and reservoirs as regulators of carbon
 921 cycling and climate, *Limnology and oceanography*, 54, 2298-2314, 2009.
 922 Tsola, S. L., Zhu, Y., Ghurnee, O., Economou, C. K., Trimmer, M., and Eyice, Ö.: Diversity
 923 of dimethylsulfide-degrading methanogens and sulfate-reducing bacteria in anoxic sediments
 924 along the Medway Estuary, UK, *Environmental Microbiology*, 23, 4434-4449, 2021.
 925 Valentine, D. L., Chidthaisong, A., Rice, A., Reeburgh, W. S., and Tyler, S. C.: Carbon and
 926 hydrogen isotope fractionation by moderately thermophilic methanogens, *Geochimica et*
 927 *Cosmochimica Acta*, 68, 1571-1590, 2004.
 928 van Grinsven, S., Meier, D. V., Michel, A., Han, X., Schubert, C. J., and Lever, M. A.: Redox
 929 zone and trophic state as drivers of methane-oxidizing bacterial abundance and community
 930 structure in lake sediments, *Frontiers in Environmental Science*, 10, 857358, 2022.
 931 van Grinsven, S., Sinninghe Damsté, J. S., Abdala Asbun, A., Engelmann, J. C., Harrison, J.,
 932 and Villanueva, L.: Methane oxidation in anoxic lake water stimulated by nitrate and sulfate
 933 addition, *Environmental microbiology*, 22, 766-782, 2020.
 934 Vekeman, B., Kerckhof, F. M., Cremers, G., De Vos, P., Vandamme, P., Boon, N., Op den
 935 Camp, H. J., and Heylen, K.: New *Methyloceanibacter* diversity from North Sea sediments
 936 includes methanotroph containing solely the soluble methane monooxygenase, *Environmental*
 937 *microbiology*, 18, 4523-4536, 2016.
 938 Veraart, A. J., Steenbergh, A. K., Ho, A., Kim, S. Y., and Bodelier, P. L.: Beyond nitrogen: the
 939 importance of phosphorus for CH_4 oxidation in soils and sediments, *Geoderma*, 259, 337-346,
 940 2015.
 941 Wang, X.-C. and Lee, C.: Sources and distribution of aliphatic amines in salt marsh sediment,
 942 *Organic Geochemistry*, 22, 1005-1021, 1994.
 943 Wang, Y., Liu, X., Wu, M., and Guo, J.: Methane-Driven Perchlorate Reduction by a Microbial
 944 Consortium, *Environmental Science & Technology*, 58, 13370-13379, 2024.



- 945 Wegener, G. and Boetius, A.: An experimental study on short-term changes in the anaerobic
946 oxidation of methane in response to varying methane and sulfate fluxes, *Biogeosciences*, 6,
947 867-876, 2009.
- 948 Wegener, G., Krukenberg, V., Riedel, D., Tegetmeyer, H. E., and Boetius, A.: Intercellular
949 wiring enables electron transfer between methanotrophic archaea and bacteria, *Nature*, 526,
950 587-590, 2015.
- 951 Wei, H., Wang, M., Ya, M., and Xu, C.: The denitrifying anaerobic methane oxidation process
952 and microorganisms in the environments: a review, *Frontiers in Marine Science*, 9, 1038400,
953 2022.
- 954 Wei, T.: i Simko V.(2021). R package'corrplot': Visualization of a Correlation Matrix.(Version
955 0.92), Available at< Available at <https://github.com/taiyun/corrplot>>. Accessed on March, 20,
956 2024.
- 957 Werne, J. P., Hollander, D. J., Lyons, T. W., and Damsté, J. S. S.: Organic sulfur
958 biogeochemistry: recent advances and future research directions, 2004.
- 959 Whiticar, M. J.: Carbon and hydrogen isotope systematics of bacterial formation and oxidation
960 of methane, *Chemical Geology*, 161, 291-314, 1999.
- 961 Xia, F., Jiang, Q.-Y., Zhu, T., Zou, B., Liu, H., and Quan, Z.-X.: Ammonium promoting
962 methane oxidation by stimulating the Type Ia methane-oxidizing bacteria in tidal flat sediments
963 of the Yangtze River estuary, *Science of the Total Environment*, 793, 148470, 2021.
- 964 Xie, Z., Li, W., Yang, K., Wang, X., Xiong, S., and Zhang, X.: Bacterial and Archaeal
965 Communities in Erhai Lake Sediments: Abundance and Metabolic Insight into a Plateau Lake
966 at the Edge of Eutrophication, *Microorganisms*, 12, 1617, 2024.
- 967 Xu, J. and Logan, B. E.: Measurement of chlorite dismutase activities in perchlorate respiring
968 bacteria, *Journal of microbiological methods*, 54, 239-247, 2003.
- 969 Yan, X., Xu, X., Wang, M., Wang, G., Wu, S., Li, Z., Sun, H., Shi, A., and Yang, Y.: Climate
970 warming and cyanobacteria blooms: Looks at their relationships from a new perspective, *Water*
971 *Research*, 125, 449-457, 2017.
- 972 Yang, R., Peng, C., Mo, Y., Kleindienst, S., Li, S., Wang, J., Kappler, A., Wang, Z., and Lu,
973 L.: Electron acceptors modulate methane oxidation and active methanotrophic communities in
974 anoxic urban wetland sediments, *Applied and Environmental Microbiology*, 91, e00386-
975 00325, 2025.
- 976 Yang, Y., Chen, J., Tong, T., Xie, S., and Liu, Y.: Influences of eutrophication on
977 methanogenesis pathways and methanogenic microbial community structures in freshwater
978 lakes, *Environmental Pollution*, 260, 114106, 2020.
- 979 Yang, Y., Chen, J., Chen, X., Jiang, Q., Liu, Y., and Xie, S.: Cyanobacterial bloom induces
980 structural and functional succession of microbial communities in eutrophic lake sediments,
981 *Environmental Pollution*, 284, 117157, 2021.
- 982 Yang, Y., Chen, J., Tong, T., Li, B., He, T., Liu, Y., and Xie, S.: Eutrophication influences
983 methanotrophic activity, abundance and community structure in freshwater lakes, *Science of*
984 *the Total Environment*, 662, 863-872, 2019.
- 985 Yvon-Durocher, G., Allen, A. P., Bastviken, D., Conrad, R., Gudas, C., St-Pierre, A., Thanh-
986 Duc, N., and Del Giorgio, P. A.: Methane fluxes show consistent temperature dependence
987 across microbial to ecosystem scales, *Nature*, 507, 488-491, 2014.
- 988 Zhao, Y., Liu, Y., Cao, S., Hao, Q., Liu, C., and Li, Y.: Anaerobic oxidation of methane driven
989 by different electron acceptors: A review, *Science of The Total Environment*, 174287, 2024.
- 990 Zhou, C., Peng, Y., Yu, M., Deng, Y., Chen, L., Zhang, L., Xu, X., Zhang, S., Yan, Y., and
991 Wang, G.: Severe cyanobacteria accumulation potentially induces methylotrophic methane
992 producing pathway in eutrophic lakes, *Environmental Pollution*, 292, 118443, 2022.



993 Zhu, Y., Chen, X., Yang, Y., and Xie, S.: Impacts of cyanobacterial biomass and nitrate
994 nitrogen on methanogens in eutrophic lakes, *Science of The Total Environment*, 848, 157570,
995 2022.
996